24th IMEKO TC4 International Symposium
22nd International Workshop on ADC and DAC Modelling and Testing
IMEKO TC-4 2020
Palermo, Italy, September 14-16, 2020

Experimental Investigation on High-Efficiency Control Algorithms for Three-phase Induction Motors

M. Caruso, A. O. Di Tommaso, R. Miceli, C. Spataro and F. Viola

Department of Engineering, University of Palermo, viale delle Scienze, Building nr. 9, 90128 - Palermo, Italy. Email: massimo.caruso16@unipa.it

***Abstract* – This paper presents an experimental investigation regarding the power losses variations occurring in three-phase induction motors (IMs) as a function of the magnetization level of the machine. More in detail, the power losses identification is obtained by changing in real-time the working operating conditions of the IM drive and the IM reference flux. The sets of measurements are carried out by setting up a test bench and the obtained results confirm that the power losses occurring in induction motors can be minimized by adequately setting the direct axis current component for each IM working condition. This research represents the starting point for the conception of advanced real-time loss model control algorithms capable of enhancing the efficiency of the IM drive.**

I. INTRODUCTION

Over the last years, the field of electric drives has faced significant innovation and improvement, thanks to the conception of new typologies of electric motors, power converters and robust control algorithms for the efficiency enhancement of the drive. Regarding the induction motor, which is very widely used both in the industry and in the automotive applications, several control techniques have been proposed in the literature, commonly classified into two categories [1,2]:

1. *Loss Model Control* (LMC), which searches the maximum efficiency by considering the IM mathematical model, including copper and iron losses, and depending on the IM parameters, such as stator and rotor resistances, magnetizing reactance and iron core equivalent resistance [3-9]. These parameters could be pre-determined through several tests (no-load, locked rotor, etc.) and assumed as constant values in the related control algorithm [10-12], or they can be estimated in real-time. The literature proposes different variables for the power loss minimization: the most commonly adopted is the magnetizing current, but several other works propose also the slip frequency [13], the slip speed [14], the magnetizing flux [7,8,15], or the stator currents [9,10].
2. *Search Control* (SC), which consists on a real-time detection of the minimum input power by iteratively changing the magnetization level of the machine for a given working condition [16-20]. One of the main drawbacks of this technique consists of oscillations in the air-gap flux, which determine torque ripples, as well as speed fluctuations. A simple technique is proposed in [21] and then improved in [22], in which the torque ripple is mitigated through feed-forward pulsating torque compensation. Other search controls adopted the Fibonacci technique [19] or variations of this method [23], avoiding the presence of the torque ripple.

In this context, it becomes crucial to accurately identify the trend of the power losses in order to determine an accurate IM loss model, accounting for iron and copper losses and considering that the parameters of the machine are sensitive to variations of temperature, saturation and frequency during the actual operation of the machine itself. Therefore, this paper presents an experimental investigation regarding the power losses variations occurring in three-phase induction motor drives as a function of the magnetization level of the machine. This research represents the starting point for the conception of advanced real-time loss model control algorithms capable of enhancing the efficiency of the IM drive. More in detail, the power losses identification is obtained by changing in real-time the working operating conditions of the drive and the IM reference flux. The sets of measurements are carried out by setting up a test bench and the experimental results confirm that the efficiency involved in IM drives can be enhanced by adequately setting a specific level of magnetization of the motor for each working condition in terms of load and speed.

The paper is structured as follows: Section II presents the equations that describe an enhanced field oriented control algorithm used for power losses identification. Section III reports the test bench equipment used for the sets of power losses measurement. Section IV discusses the experimental results carried out for the proposed investigation.

II. EQUATIONS OF THE FIELD ORIENTED CONTROL ALGORITHM

The Field Oriented Control (FOC) strategy has been taken into account as the algorithm for the power losses identification. More specifically, the corresponding IM model is depicted in Fig. 1.

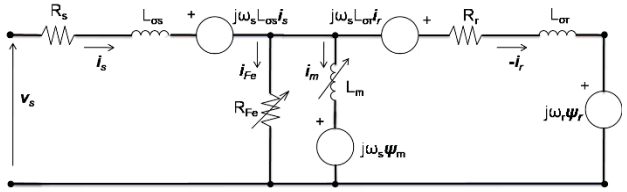

Fig. 1. The IM equivalent circuit.

The equations governing the electrical and mechanical balances are given by:

$$T_{\sigma r}\frac{d\psi_{rd}}{dt}+\psi_{rd}=\psi_{md} \tag{1}$$

$$\omega_s=\frac{d\theta_s}{dt}=\frac{T_{\sigma r}}{\psi_{mq}}\psi_{rd}+\omega_r \tag{2}$$

$$T_{\sigma Fe}\frac{d\psi_{md}}{dt}+\psi_{md}=L_{\sigma r}(i_{sd}-i_{md})+\psi_{rd}+T_{\sigma Fe}\omega_s\psi_{mq} \tag{3}$$

$$T_{\sigma Fe}\frac{d\psi_{mq}}{dt}+\psi_{mq}=L_{\sigma r}(i_{sq}-i_{mq})-T_{\sigma Fe}\omega_s\psi_{md} \tag{4}$$

$$T_{em}=\frac{3}{2}p\frac{1}{L_{\sigma r}}\psi_{md}\psi_{mq}=K_T\psi_{md}\psi_{mq} \tag{5}$$

where ψ_{rd} and ψ_{rq} are the direct-axis and quadrature-axis rotor flux components, respectively, ω_r and ω_s represent the rotor speed and the synchronous speed, respectively, θ_s is the rotor flux angular position, i_{sd} and i_{sq} are the direct-axis and quadrature-axis stator current components, respectively, L_m is the magnetizing inductance, R_{Fe} is the core loss resistance, R_r and $L_{\sigma r}$ are the rotor resistance and the rotor leakage inductance, respectively, $T_{\sigma r}=L_{\sigma r}/R_r$ and $T_{\sigma Fe}=L_{\sigma r}/R_{Fe}$ are rotor time constants, T_{em} is the electromagnetic torque and p is the number of pole pairs.

The FOC condition is taken into account by considering the following formula:

$$\frac{d\psi_{rq}}{dt}=\psi_{rq}=0 \tag{6}$$

The direct-axis and quadrature-axis magnetizing current components, namely i_{md} and i_{mq}, can be determined as

$$i_{md}=i_m\frac{\psi_{md}}{\psi_m} \tag{7}$$

$$i_{mq}=i_m\frac{\psi_{mq}}{\psi_m} \tag{8}$$

where

$$\psi_m=\sqrt{\psi_{md}^2+\psi_{mq}^2} \tag{9}$$

The non-linearity of the magnetic material is considered by taking into account the magnetizing curve i_m =f (ψ_m) depicted in Fig. 2, obtained from a no-load test at synchronous speed and whose fitting is given by the following equation:

$$i_m=119.6\psi_m^6+250.8\psi_m^5+181.7\psi_m^4\backslash-44.92\psi_m^3-0.83\psi_m^2+4.43\psi_m \tag{10}$$

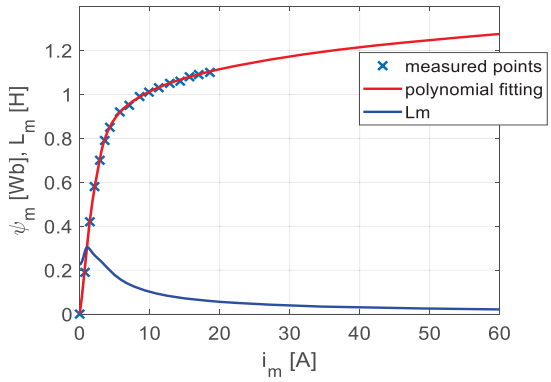

Fig. 2. Magnetizing curve and actual trend of the magnetizing inductance L_m.

The simplified scheme of the FOC algorithm, which implements (6-10), is shown in Fig. 3. In the torque control channel, the output IM position is compared with the reference position θ_{ref} and the error is processed by a PI controller in order to provide the reference speed ω_{ref}, which is, then, compared with the IM output speed. The speed error is processed by the PI, providing the reference q -axis current, i_{sq}^* , which is compared with the i_{sq} current of the motor. The determined error provides the reference q -axis voltage v_{sq}^*, needed for the motor supply. In the magnetization control channel, the reference flux is compared with the IM rotor flux. The error processed by the PI provides the reference direct-axis current component, i_{sd}^*, and the current of the IM, namely i_{sd}, determines the reference d -axis voltage v_{sd}^*. Finally, the decoupled v_{sd}^* and v_{sq}^* signals are sent to the Space Vector Modulation block, providing the input quantities for the inverter.

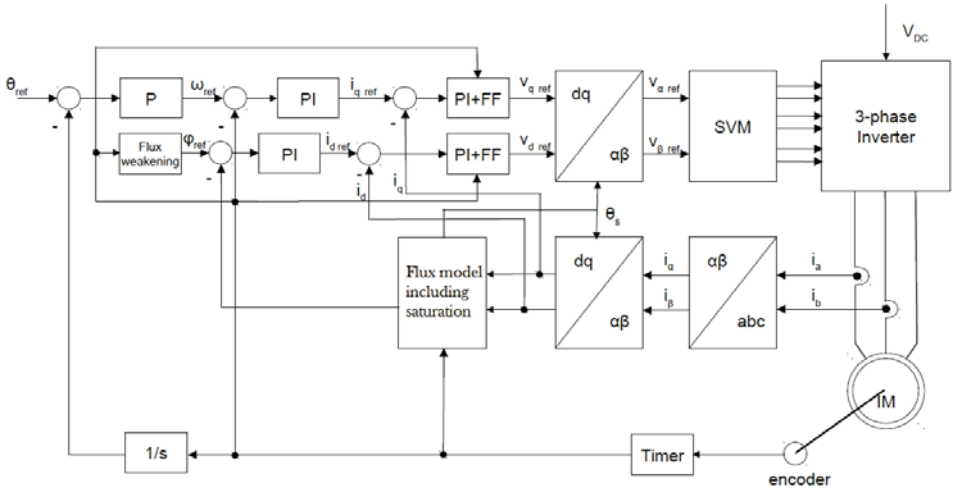

Fig. 3. Block scheme of the IM control system.

III. TEST BENCH SETUP

A test bench has been set-up for the experimental power loss identification. Fig. 4 shows the schematic representation of the bench, which is composed by:

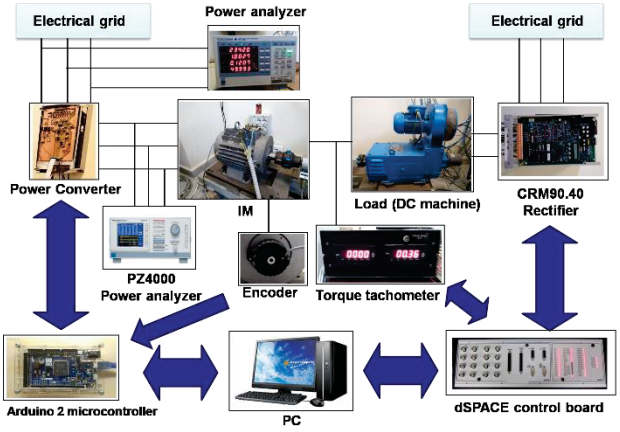

Fig. 4. Schematic representation of the test bench.

- A 5.5 kW three-phase, double squirrel-cage rotor, induction machine, depicted in Fig. 5, whose rated values and parameters are summarized in Table I.
- A SINUS-IFDE power converter (*Elettronica Santerno Inc.*) for the IM power supply. The converter is controlled with a Space Vector Pulse Width Modulation technique with a switching frequency equal to 10.25 kHz.
- An incremental encoder (*Eltra Inc., model EH80*) for the IM position and speed measurements.
- A 7.83 kW DC machine (*Stipaf Elettromeccanica*), which emulates the IM applied load. The machine is supplied by a CRM90.40 converter (*Elettronica Santerno*).
- A low-cost ATMEL ATSAM3X8E, ARM type, microcontroller, mounted on an "Arduino Due" board, running at a clock frequency of 84 MHz, for the experimental implementation of the enhanced field oriented control algorithm. The speed of the IM is also controlled by the Arduino Due micro-controller [24].
- A PZ4000 power analyzer (*Yokogawa Inc.*) for the real-time acquisition of the *rms* values of both voltages and current.
- A dSPACE user interface for the real-time control of the armature current of the DC machine.

Fig. 5. The three-phase induction motor under test.

Table 1. Main rated values and parameters of the IM under test.

Quantity	Value
Power [kW]	5.5
Voltage [V]	400
Current [A]	13
Frequency [Hz]	50
Torque [Nm]	18
Rated speed [rpm]	2850
Stator resistance [Ω]	0.56
Rotor resistance [Ω]	0.77
Stator inductance [H]	0.116
Rotor inductance [H]	0.119
Rated rotor flux [Wb]	0.9

A photograph of the test bench is shown in Fig. 6.

Fig. 6. A photograph of the test bench.

IV. EXPERIMENTAL RESULTS

The experimental investigation has been carried out by means of the test bench described in Section III. More specifically, the IM working conditions have been varied by setting the reference speed in a range between 50 and 300 rad/s, with steps of 50 rad/s, and the applied load from 0% to its rated load, with steps of 10%. For each condition, the reference flux has been varied within the range of 0.1 Wb ÷ 1 Wb with steps of 0.1 Wb. The input power, the voltages and the currents have been measured through the power analyzer with an averaging set at 64 measurements. For each working point, the input power has been measured within a window equal to 1 minute. In addition, in order to improve the related accuracy, each measurement has been repeated ten times. Thus, for each working condition, this search control is capable of determining the optimal flux value (corresponding to the optimal direct-axis current component) that minimizes the input power (i.e., the power losses), enhancing, therefore, the efficiency of the whole drive.

For instance, Fig. 7 shows the results in terms of search control for ω_{ref}=150 rad/s at 50% of the rated load. As well as for the simulation results, it can be noticed that the trend of the input power can be minimized by acting on the magnetization level of the machine.

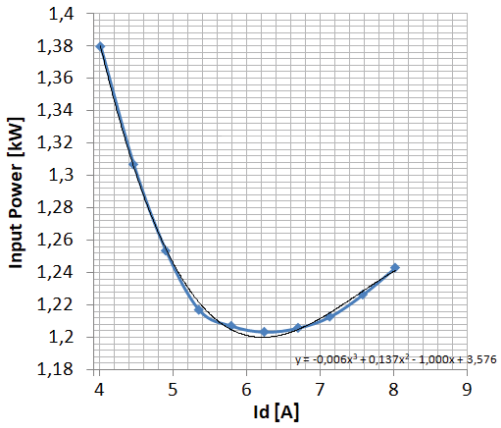

Fig. 7. Search control for ω_{ref} = 100 [rad/s] and T=50%.

Similar results are obtained by parameterizing the values of the applied torque, as shown in Figs. 8 and 9, depicting the search control procedure for ω_{ref} equal to 300 rad/s and 200 rad/s, respectively. For all of the working conditions, it can be noticed that the minimum values of power losses is detected for different values of the IM magnetization level. More specifically, the minimum values of input power slide towards lower values of I_d and the condition of minimum power losses appears to be almost independent from the speed condition. In any case, the experimental results confirm that the power losses involved in the IM drive can be minimized by adequately acting on the magnetization level of the machine.

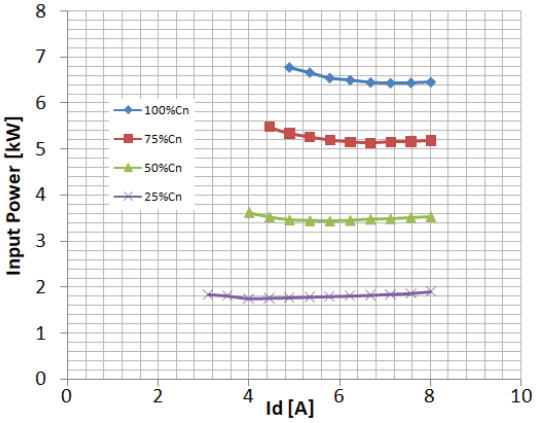

Fig. 8. Search control for ω_{ref} = 300 [rad/s].

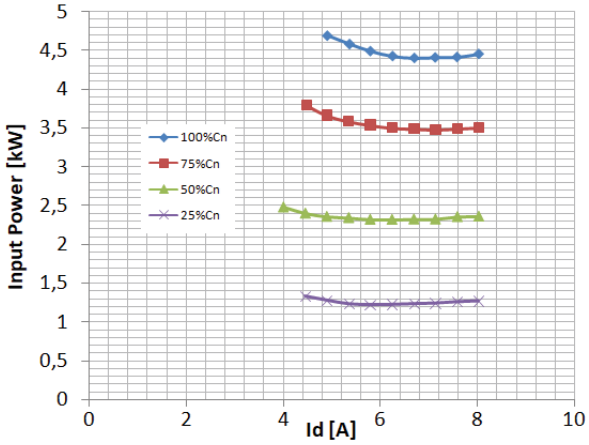

Fig. 9. Search control for ω_{ref} = 200 [rad/s].

Other interesting results are shown in Fig. 10, depicting the trends of I_q as a function of I_d parameterized for 4 conditions of applied load (25%, 50%, 75% and 100% of rated load) and 3 conditions of IM speed (100 rad/s, 200 rad/s and 300 rad/s). From this point of view, it can be noticed that the locus of the optimal $I_d - I_q$ pairs that minimizes the input power covers an exponential trend, which is obtained by connecting the points of minimum losses for each working condition. The implementation of this exponential trend in high-performance control algorithms can certainly improve the efficiency of the whole drive.

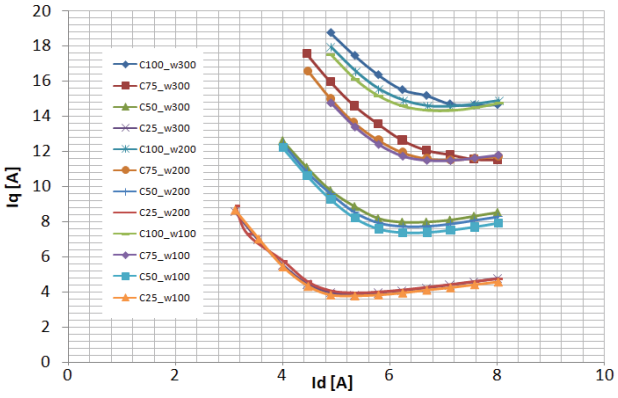

Fig. 10. $I_d - I_q$ region for the minimum power loss identification.

V. CONCLUSIONS

This work has described an experimental investigation aimed at determining the power loss identification in three-phase induction machines for innovative loss model algorithms, capable of enhancing the efficiency of the electrical drive. Several working conditions have been proposed by implementing an enhanced dynamic model of the machine and by setting up an experimental IM test bench. The obtained results are confirmed by an extended set of measurements carried out on a 5.5 kW induction machine by varying the working conditions of the motor and its magnetization level. The results obtained from this investigation have demonstrated the fact that the power losses involved in the whole drive can be minimized by adequately setting the reference flux on the FOC algorithm for each working condition in terms of load and speed.

ACKNOWLEDGMENTS

This work was financially supported by PON R&I 2015-2020 “Propulsione e Sistemi Ibridi per velivoli ad ala fissa e rotante – PROSIB”, CUP no:B66C18000290005, by H2020-ECSEL-2017-1-IA-two-stage “first and european sic eightinches pilot line-REACTION”, by Prin 2017-Settore/Ambito di intervento: PE7 linea C - Advanced power-trains and -systems for full electric aircrafts, by PON R&I 2014-2020 - AIM (Attraction and International Mobility), project AIM1851228-1 and by ARS01_00459-PRJ-0052 ADAS+ “Sviluppo di tecnologie e sistemi avanzati per la sicurezza dell'auto mediante piattaforme ADAS”.

REFERENCES

[1] A. M. Bazzi and P. T. Krein, “Review of methods for real-time loss minimization in induction machines,” IEEE Transactions on Industry Applications, vol. 46, pp. 2319–2328, Nov 2010.

[2] S. Kumar and K. Vasanthkumar, “Energy efficient control of three-phase induction motor,” International Journal of Computing Algorithm, vol. 1, pp. 48–54, dec 2012.

[3] C. Chakraborty and Y. Hori, “Fast efficiency optimization techniques for the indirect vector-controlled induction motor drives,” IEEE Transactions on Industry Applications, vol. 39, pp. 1070–1076, July 2003.

[4] F. Fernandez-Bernal, A. Garcia-Cerrada, and R. Faure, “Model-based loss minimization for dc and ac vector-controlled motors including core saturation,” IEEE Transactions on Industry Applications, vol. 36, pp. 755–763, May 2000.

[5] S. Vaez-Zadeh and F. Hendi, “A continuous efficiency optimization controller for induction motor drives,” Energy Conversion and Management, vol. 46, no. 5, pp. 701 – 713, 2005.

[6] A. Bruno, M. Caruso, A. O. D. Tommaso, C. Nevoloso, and R. Miceli, “Experimental comparison of efficiency enhancement algorithms for three-phase induction motors,” in 2019 Fourteenth International Conference on Ecological Vehicles and Renewable Energies (EVER), pp. 1–6, May 2019.

[7] D. Spirov, “Optimal algorithms for minimizing of active and reactive power of induction motors taking into account of iron losses,” in 2019 16th Conference on Electrical Machines, Drives and Power Systems (ELMA), pp. 1–4, June 2019.

[8] Z. Qu, M. Ranta, M. Hinkkanen, and J. Luomi, “Loss-minimizing flux level control of induction motor drives,” IEEE Transactions on Industry Applications, vol. 48, no. 3, pp. 952–961, 2012.

[9] Jianqiang Liu, Xiaojie You, and T. Q. Zheng, “Efficiency optimal control in braking process for linear metro,” in 2010 5th IEEE Conference on Industrial Electronics and Applications, pp. 1363–1367, June 2010.

[10] M. N. Uddin and S. W. Nam, “New online loss-minimization-based control of an induction motor drive,” IEEE Transactions on Power Electronics, vol. 23, pp. 926–933, March 2008.

[11] I. Kioskeridis and N. Margaris, “Loss minimization in induction motor adjustable-speed drives,” IEEE Transactions on Industrial Electronics, vol. 43, pp. 226–231, Feb 1996.

[12] G. O. Garcia, J. C. M. Luis, R. M. Stephan, and E. H. Watanabe, “An efficient controller for an adjustable speed induction motor drive,” IEEE Transactions on Industrial Electronics, vol. 41, pp. 533–539, Oct 1994.

[13] A. Mannan, T. Murata, J. Tamura, and T. Tsuchiya, “Efficiency optimized speed control of field oriented induction motor including core loss,” in Proceedings of the Power Conversion Conference-Osaka 2002 (Cat. No.02TH8579), vol. 3, pp. 1316–1321 vol.3, April 2002.

[14] M. Cacciato, A. Consoli, G. Scarcella, G. Scelba, and A. Testa, “Efficiency optimization techniques via constant optimal slip control of induction motor drives,” in International Symposium on Power Electronics, Electrical Drives, Automation and Motion, 2006. SPEEDAM 2006., pp. 33–38, 2006.

[15] E. Poirier, M. Ghribi, and A. Kaddouri, “Loss minimization control of induction motor drives based on genetic algorithms,” in IEMDC 2001. IEEE International Electric Machines and Drives Conference (Cat. No.01EX485), pp. 475–478, June 2001.

[16] B. K. Bose, N. R. Patel, and K. Rajashekara, “A neuro-fuzzy-based online efficiency optimization control of a stator flux-oriented direct vectorcontrolled induction motor drive,” IEEE Transactions on Industrial Electronics, vol. 44, pp. 270–273, April 1997.

[17] D. S. Kirschen, D. W. Novotny, and T. A. Lipo, “On-line efficiency optimization of a variable frequency induction motor drive,” IEEE Transactions on Industry Applications, vol. IA-21, pp. 610–616, May 1985.

[18] P. Famouri and J. J. Cathey, “Loss minimization control of an induction motor drive,” IEEE Transactions on Industry Applications, vol. 27, pp. 32–37, Jan 1991.

[19] Gyu-Sik Kim, In-Joong Ha, and Myoung-Sam Ko, “Control of induction motors for both high dynamic performance and high power efficiency,” IEEE Transactions on Industrial Electronics, vol. 39, pp. 323–333, Aug 1992.

[20] J. C. Moreira, T. A. Lipo, and V. Blasko, “Simple efficiency maximizer for an adjustable frequency induction motor drive,” IEEE Transactions on Industry Applications, vol. 27, pp. 940–946, Sep. 1991.

[21] D. S. Kirschen, D. W. Novotny, and T. A. Lipo, “Optimal efficiency control of an induction motor drive,” IEEE Transactions on Energy Conversion, vol. EC-2, pp. 70–76, March 1987.

[22] G. C. D. Sousa, B. K. Bose, and J. G. Cleland, “Fuzzy logic based on-line efficiency optimization control of an indirect vector-controlled induction motor drive,” IEEE Transactions on Industrial Electronics, vol. 42, pp. 192–198, April 1995.

[23] Cao-Minh Ta and Y. Hori, “Convergence improvement of efficiencyoptimization control of induction motor drives,” IEEE Transactions on Industry Applications, vol. 37, no. 6, pp. 1746–1753, 2001.

[24] V. Castiglia, P. Ciotta, A. O. Di Tommaso, R. Miceli, and C. Nevoloso, “High performance foc for induction motors with low cost atsam3x8e microcontroller,” in 2018 7th International Conference on Renewable Energy Research and Applications (ICRERA), pp. 1495–1500, Oct 2018.